AIAA 80-1566R

Departure Susceptibility and Uncoordinated Roll-Reversal Boundaries for Fighter Configurations

William Bihrle Jr.* and Billy Barnhart†
Bihrle Applied Research, Inc., Jericho, New York

A fighter's response to a severe application of controls is predicted as a function of its static lateral and directional stability derivatives and lateral control characteristics. This was accomplished by developing two boundaries which identify the onset of roll reversal and departure in terms of the lateral-directional characteristics. These boundaries demark four airplane response regions, i.e., commanded maneuver, commanded maneuver accompanied by an alpha excursion, uncoordinated roll reversal, and departure susceptibility. The responses within the latter two regions become progressively more severe the further the lateral-directional characteristics are displaced from the onset boundary values. The boundaries were developed and their sensitivity to other variables was determined through large-angle, six-degree-of-freedom parametric computer studies. Since they were found to be applicable for most fighter mass distributions and for a large range of pitch characteristics, it was concluded that they could be used for specification, design, and evaluation purposes.

Nomenclature

b	= wing span, ft
C_l	= rolling-moment coefficient
C_n	= yawing-moment coefficient
C_{l_β}	= lateral-stability derivative, deg^{-1}
$C_{l_{\delta_a}}$	= roll due to lateral control derivative, deg^{-1}
$C_{m_{\|\beta\|}}$	= pitch due to sideslip derivative, deg^{-1}
C_{n_β}	= directional-stability derivative, deg^{-1}
$C_{n_{\beta_{DYN}}}$	= dynamic directional-stability parameter $= C_{n_\beta}\cos\alpha - (I_z/I_x)C_{l_\beta}\sin\alpha$
$C_{n_{\delta_a}}$	= yaw due to lateral control derivative, deg^{-1}
C_{m_q}	= pitch-damping derivative, rad^{-1}
i_s	= longitudinal control deflection, deg
I_x, I_y, I_z	= moment of inertia about the x-, y-, and z-body axis, respectively, slug-ft^2
$(I_x - I_y)/mb^2$	= inertia yawing-moment parameter
$(I_y - I_z)/mb^2$	= inertia rolling-moment parameter
$(I_z - I_x)/mb^2$	= inertia pitching-moment parameter
m	= mass, slug
LCDP	= lateral control departure parameter $= C_{n_\beta} - (C_{n_{\delta_a}}/C_{l_{\delta_a}})C_{l_\beta}$
α	= angle of attack, deg
β	= sideslip angle, deg

Introduction

HIGH-angle-of-attack capability in the post stall region has been shown[1] to significantly enhance the air combat maneuvering effectiveness of fighter airplanes. Unfortunately, it has not been possible to design for such a capability with a modicum of confidence since departure from controlled flight could not be analytically predicted. The departure motion of concern is one in which the pilot has lost complete control due to an unanticipated yawing motion which occurs so quickly that the airplane is in a post stall gyration, or an incipient spin, before he can take corrective action. This yawing motion can be triggered by vortex shedding asymmetrically from the fuselage forebody or through use of the lateral control.

Presented as Paper 80-1566 at the AIAA 7th Atmospheric Flight Mechanics Conference, Danvers, Mass., Aug. 11-13, 1980; submitted Oct. 3, 1980; revision received Feb. 24, 1982.

*President. Associate Fellow AIAA.
†Chief Engineer.

Asymmetric vortex shedding through some post stall angle-of-attack range generates a significant aerodynamic yawing moment at zero sideslip, whereas the yawing motion generated during a rolling maneuver depends on the aerodynamic characteristics of the lateral control as well as the large-angle stability of the airframe. Regardless of the trigger mechanism, the nature of the ensuing motion is largely a function of the aerodynamic characteristics experienced in a rotational flow environment, e.g., the damping or autorotative rolling and yawing moments generated as a function of rate of rotation. Consequently, static aerodynamic data can only predict the *susceptibility* to depart, but not the departure motion itself. (Only very recently has a viable rotary balance testing facility[2] become available for ascertaining the influence of airplane configurations on the rotational flow aerodynamics.)

The presence of a static yawing moment at zero sideslip is in itself indicative of departure susceptibility. Departure susceptibility induced by a rolling maneuver, however, depends on the relative magnitude of several key static aerodynamic parameters and their variation with angle of attack, as well as the airframe's inertial characteristics. These key parameters were identified during previous analytical and experimental investigations. For example, an analytical study[3] showed that adverse yaw due to lateral control deflection, dihedral effect, and directional stability were instrumental in spin development. These same parameters have also been addressed in existing departure criteria, i.e., LCDP[4] and $C_{n_{\beta_{DYN}}}$. In efforts to minimize departure susceptibility and enhance handling qualities at high alphas, investigators[5] in recent years have sought to maintain positive values for both these criteria to as high an angle of attack as possible. Boundaries for identifying departure characteristics that relate these criteria to each other have also been proposed.[6]

Since lateral control induced departure is a high-angle-of-attack motion in which both inertial and kinematic coupling generate large uncommanded alpha and beta excursions, limited degree-of-freedom linearized equations of motions cannot model this phenomenon. Consequently, criteria based on simplified equations cannot be expected to accurately predict a specific configuration's departure susceptibility, though they may serve as valuable preliminary design guides.

Efforts[7,8] were made to identify accurately a fighter's susceptibility to depart from controlled flight during a high-angle-of-attack rolling maneuver by examining the airframe's

large-angle stability. A large-angle, six-degree-of-freedom digital computer program was utilized to simulate the motions of a fighter performing a severe air combat maneuver for combinations of the previously discussed static lateral-directional parameters. The simulation was repeated for several inertial and pitching-moment characteristics to determine their effect. Resulting time histories were employed to generate design charts. These charts served as the basis for developing boundaries which identify departure susceptibility and uncoordinated roll-reversal flight characteristics as functions of the lateral-directional parameters being studied.

Technical Approach

Inertial and Aerodynamic Models

The technical approach was to generate design charts and boundaries based on a parametric study, instead of deriving a closed-form analytical solution. This approach was predicated on ascertaining that a reasonable number of inertial and aerodynamic (C_l, C_n, and $C_{n_{\delta_a}}$) models could represent the spectrum of fighter-type airplanes.

Figure 1 shows that the distribution of the mass within the fuselage is the same for all fighters as demonstrated by their constant $(I_y - I_z)/mb^2$ inertia parameter values. Also, since the $(I_x - I_y)/mb^2$ inertia parameter value is always negative, it is shown that the mass is more heavily concentrated in the fuselage than the wing, although to varying degrees. Consequently, two inertia parameter models, i.e., *A* and *C*, encompass all fighter values. A preliminary investigation indicated that the boundary information generated with inertia parameter model *B* would be substantially the same as with model *A*, and, in most instances, with model *C*. To significantly reduce the number of cases to be examined, and since model *B* represented most fighters, model *B* was chosen to be used extensively for this investigation.

In order to select representative C_l, C_n, and $C_{n_{\delta_a}}$ models, high-angle-of-attack, high Reynolds number data were collected for fighter-type airplanes developed in this country over the past 25 years. It was found that all the data fell into broad bands throughout the angle-of-attack range, so that it was possible to represent these aerodynamic characteristics for the spectrum of fighter-type airplanes with a reasonable number of models, i.e., four C_l, three C_n, and three $C_{n_{\delta_a}}$ models, as presented in Figs. 2-4, respectively. While the models do not represent specific airplanes, they do encompass the aerodynamic characteristics of fighter-type airplanes.

Design charts and boundaries were developed for these lateral-directional aerodynamic models using one representative set of pitch characteristics, referred to in Figs. 5-7 as the basic model. To determine the extent to which changing the pitching moment characteristics would modify the resulting boundaries, the static stability, C_{m_q}, and $C_{m_{|\beta|}}$ were varied, as shown in Figs. 5-7, respectively.

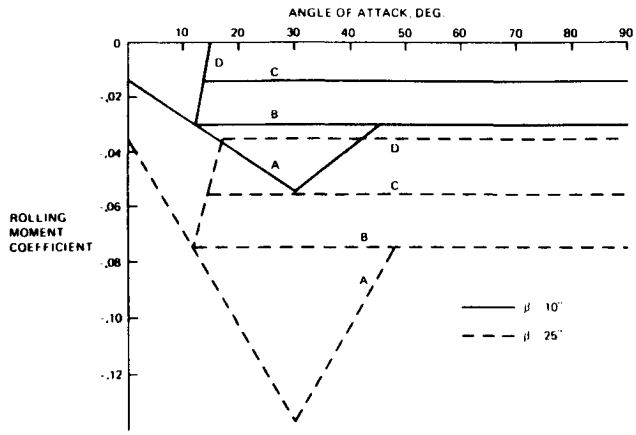

Fig. 1 Rolling-moment coefficient models.

Airplane Time Responses

Large-angle, six-degree-of-freedom time histories were generated for all possible combinations of the C_l, C_n, and $C_{n_{\delta_a}}$ models using the basic pitching moment model. This procedure was repeated for each of the pitching-moment parameter models. For this pitch study, however, only the adverse $C_{n_{\delta_a}}$ model was considered, since it is characteristic of most lateral controls at high angles of attack.

The airplane was trimmed in a 60-deg bank-angle turn at 35,000 ft and Mach 0.9. A rolling pull-out maneuver was then

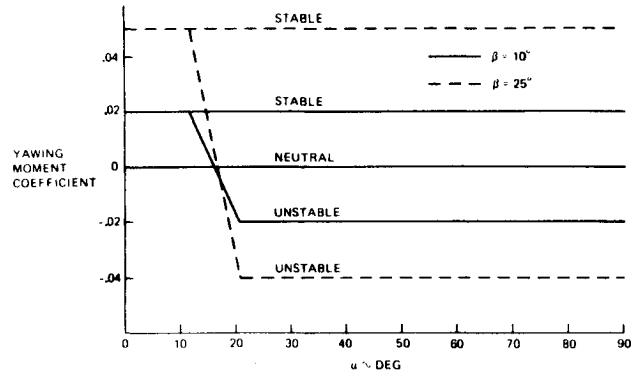

Fig. 2 Yawing-moment coefficient models.

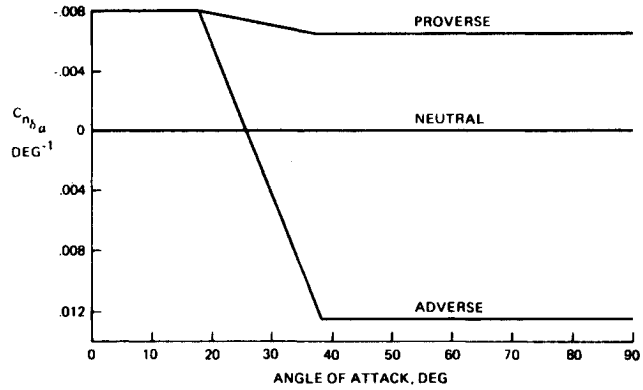

Fig. 3 Yawing moment due to lateral control derivative, $C_{n_{\delta_a}}$, models.

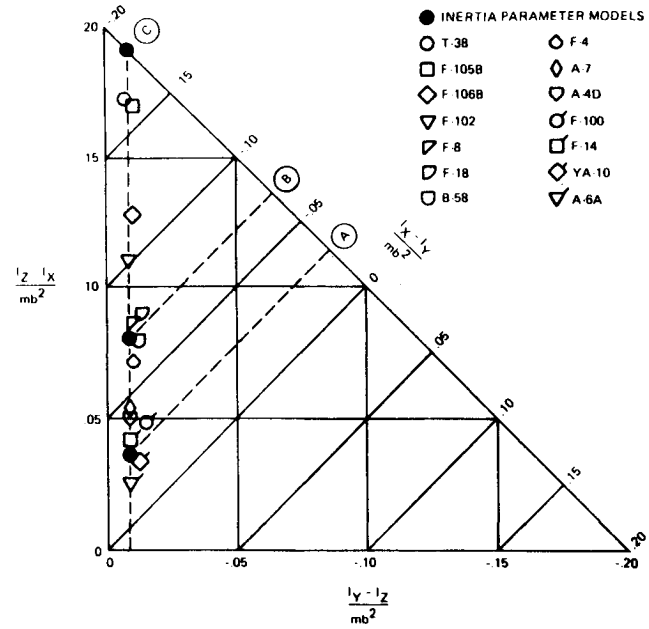

Fig. 4 Inertia parameter models.

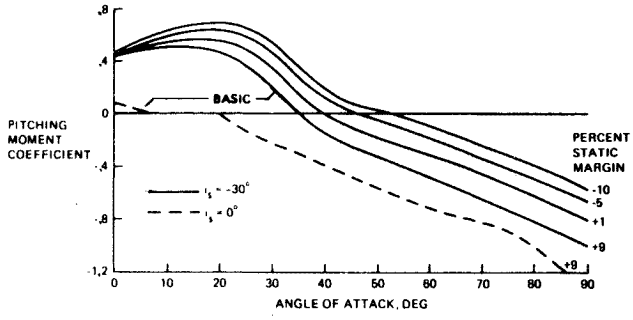

Fig. 5 Pitching-moment coefficient as a function of angle of attack for various static margins.

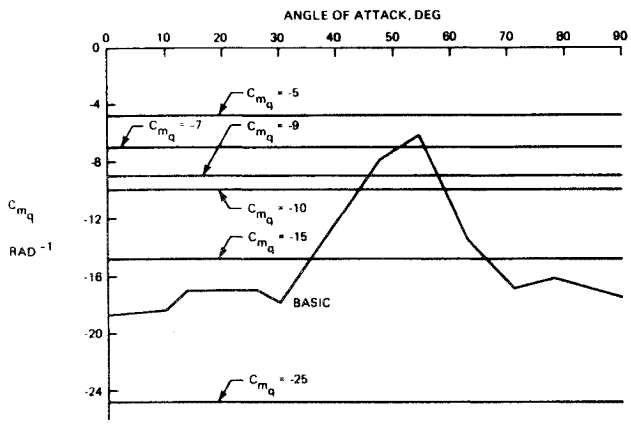

Fig. 6 Pitch-damping derivative, C_{m_q}, models.

performed in which the controls were fully deflected such that the airplane pitched up rapidly through the stall and, being uncoordinated, experienced large sideslip angles. This severe air combat maneuver was chosen because it would result in the most stringent departure boundary. Control inputs for the maneuver were

1) Full trailing-edge-up longitudinal control deflection at 30 deg/s.

2) Full lateral control deflection initiated 1.5 s into the maneuver at a rate of 30 deg/s in the direction to unbank the airplane.

3) Rudder undeflected.

The controls were kept fully deflected for a duration sufficient to allow the airplane motions to develop, at which time both the longitudinal and lateral controls were returned to trim at 30 deg/s.

Design Charts

The time-history traces were examined to determine the influence of each aerodynamic parameter on the ensuing airplane motions. To analyze the results, various time-history parameters considered to be significant indicators of these motions were tabulated. Of these time-history parameters, the third peak of the angle-of-attack time-history, peak yaw rate magnitude and sign, as well as incremental peak bank angle prior to lateral control removal were found to be most useful in defining the airplane motions and, hence, in developing boundaries.

Design charts presented these time-history parameters as functions of the studied lateral-directional models. An airplane's tendency to depart from controlled flight or to experience an uncoordinated roll reversal was predicted by studying this information.

Boundaries

In order to develop departure susceptibility boundaries, some criterion must be established either to define the point at

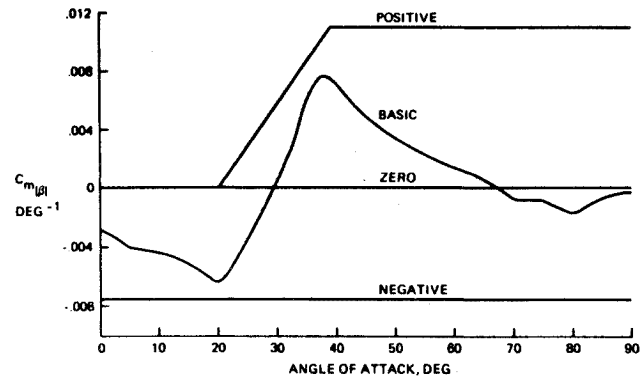

Fig. 7 Pitching-moment cross derivative, $C_{m_{|\beta|}}$, models.

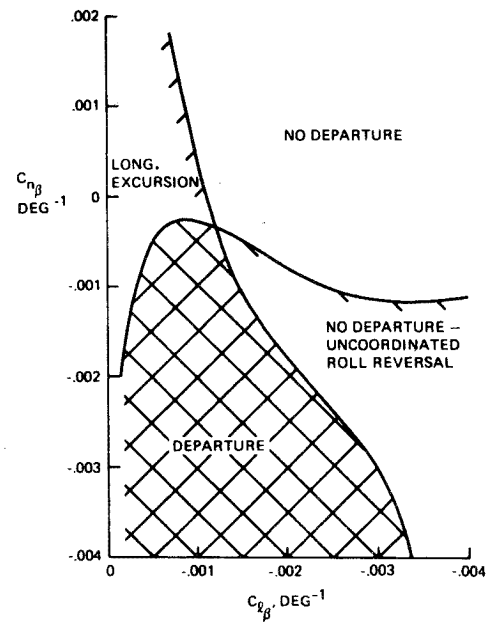

Fig. 8 Departure susceptibility and uncoordinated roll-reversal boundaries for fighter configurations having proverse $C_{n_{\delta_a}}$.

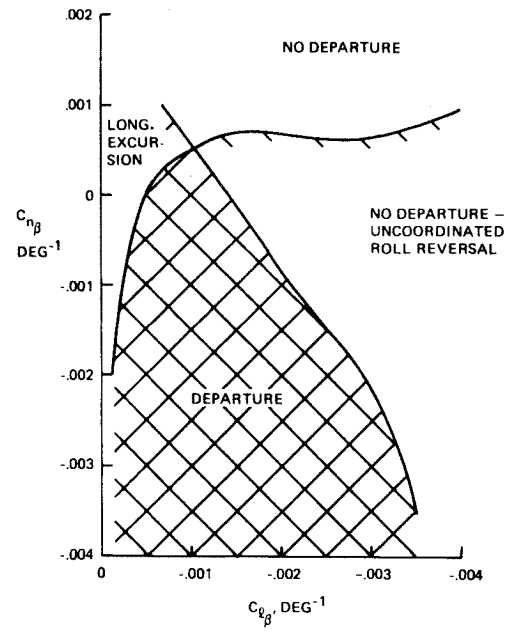

Fig. 9 Departure susceptibility and uncoordinated roll-reversal boundaries for fighter configurations having neutral $C_{n_{\delta_a}}$.

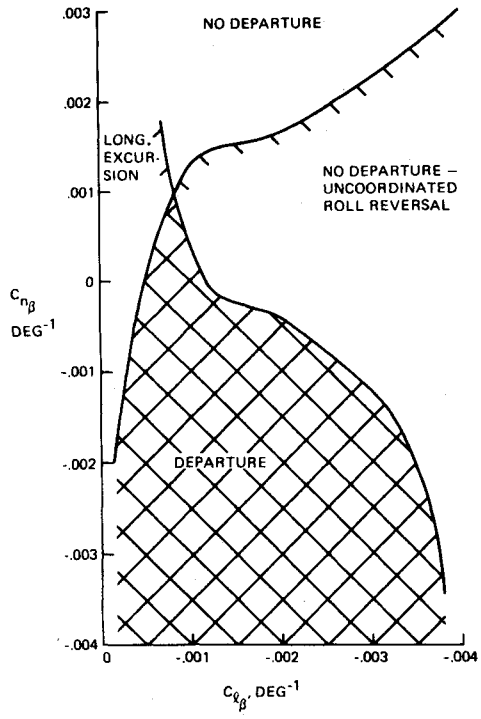

Fig. 10 Departure susceptibility and uncoordinated roll-reversal boundaries for fighter configurations having adverse $C_{n_{\delta_a}}$.

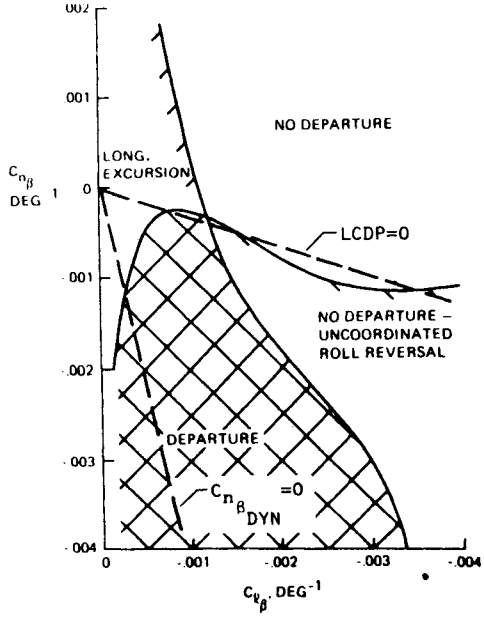

Fig. 11 Comparison of boundaries to LCDP and $C_{n_{\beta_{DYN}}}$ criteria for proverse $C_{n_{\delta_a}}$. $C_{n_{\beta_{DYN}}}$ based on $(I_z/I_x)=6$ and $\alpha=35$ deg.

which a departure has occurred, or to indicate that a departure is imminent. Since these investigations did not include a rotary aerodynamic model, as mentioned previously, it was not possible to predict actual departure and incipient spin motions. However, it was possible, with the aerodynamics as modeled herein to identify excursions into the angle-of-attack region where autorotative rolling and yawing moments, if present, could induce spins.

For many combinations of the lateral-directional aerodynamic models investigated, the yaw rates were opposite to the commanded lateral control displacements and were accompanied by a roll reversal. Consequently, the airplane

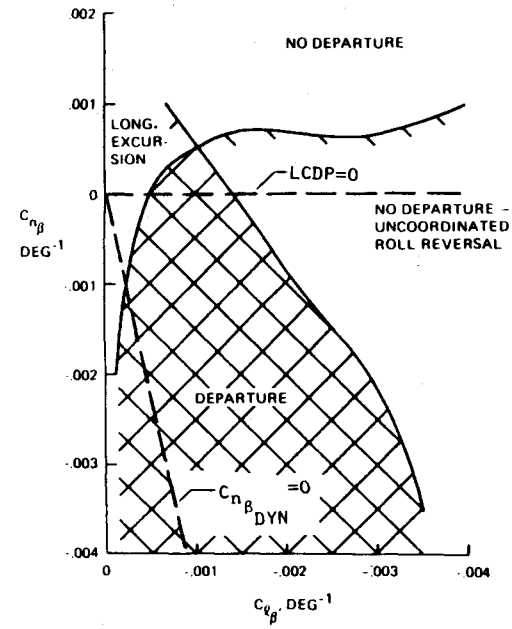

Fig. 12 Comparison of boundaries to LCDP and $C_{n_{\beta_{DYN}}}$ criteria for neutral $C_{n_{\delta_a}}$. $C_{n_{\beta_{DYN}}}$ based on $(I_z/I_x)=6$ and $\alpha=35$ deg.

rolled in the same direction that it yawed, but contrary to command. It was decided that an uncoordinated roll-reversal boundary be defined by the lateral-directional values which resulted in the airplane just returning to level flight as commanded. Consequently, in the roll-reversal region immediately below this boundary (see Figs. 8-10), the airplane's yawing and rolling motions are not particularly violent, and coupling effects do not elevate the angle of attack significantly above its high-alpha trim point. An airplane exhibiting these characteristics would not be departure prone. Also, the roll response would present a strong signal to the pilot to coordinate the maneuver or to depress the angle of attack, thus maintaining controlled flight.

As the lateral-directional characteristics are varied deeper into the roll-reversal region, however, the motions become progressively more severe, accompanied by larger-angle-of-attack excursions. At some point, the motions are so severe that the pilot would be incapable of "entering the loop" in time to prevent an incipient spin motion. At that point, a departure has occurred.

Thus two sets of boundaries can be established: one defining an uncoordinated roll reversal; another defining departure susceptibility. The criterion chosen to indicate departure susceptibility was based on the angle-of-attack time history: if the third peak of the angle-of-attack trace, following control application, were greater than 15 deg above the high-angle-of-attack trim point, the configuration was considered to be departure susceptible. This choice was based, partly, on examining flight test time histories over many years. It was observed that this criterion was usually indicative of the ensuing motion.

As the aerodynamic parameters are varied below the departure susceptibility boundary, the airplane motions in response to the control inputs continue to become increasingly more severe. It is recognized that the control inputs chosen for this study result in a stringent boundary, by design. Using a less aggressive control manipulation, an airplane having high-angle-of-attack characteristics indicative of departure susceptibility may "beat" the specified boundary. This, however, does not preclude the potential for departure in response to a more severe maneuver.

Results and Discussion

Boundaries

For ease of use, the uncoordinated roll-reversal and departure susceptibility boundaries are presented in terms of derivatives, i.e., C_{l_β}, C_{n_β}, which are the post stall slopes taken between $\beta = 0$ and 10 deg. Figures 8-10 present composite plots of these boundaries for the proverse, neutral, and adverse $C_{n_{\delta_a}}$ models, respectively. From these plots, it can be seen that there are four regions defining the airplane responses:

1) The region labeled "No Departure" lying above both the departure and uncoordinated roll-reversal boundaries indicates that for C_{n_β}, C_{l_β} combinations in this region, no high-angle-of-attack excursions are experienced and the airplane rolls and yaws as commanded.

2) The region labeled "No Departure—Uncoordinated Roll Reversal," which lies between the two boundaries, indicates that the airplane is not departure susceptible in this region, as defined herein, but that without a coordinating rudder input, the airplane will roll and yaw opposite to command.

3) The region labeled "Departure" indicates that the airplane will be departure susceptible in this region.

4) The final region, which extends along the left side of the figures above the uncoordinated roll reversal boundary and below the departure susceptibility boundary, represents a high-angle-of-attack excursion region. The airplane would roll as commanded, accompanied normally by only small yaw rates, but would be apt to experience higher angles of attack than would be anticipated.

It must be recognized that the identified responses vary within each of these regions. An airplane's response would progressively deteriorate if the C_{l_β}, C_{n_β} values were varied in a clockwise direction from the "No Departure" region. The roll response would diminish until the uncoordinated roll-reversal boundary was crossed; below the boundary, roll reversals would be experienced. Varying the C_{l_β}, C_{n_β} values further would produce increasingly more severe roll reversals, until departures would occur. Further variations into the departure region would result in even more severe departure motions.

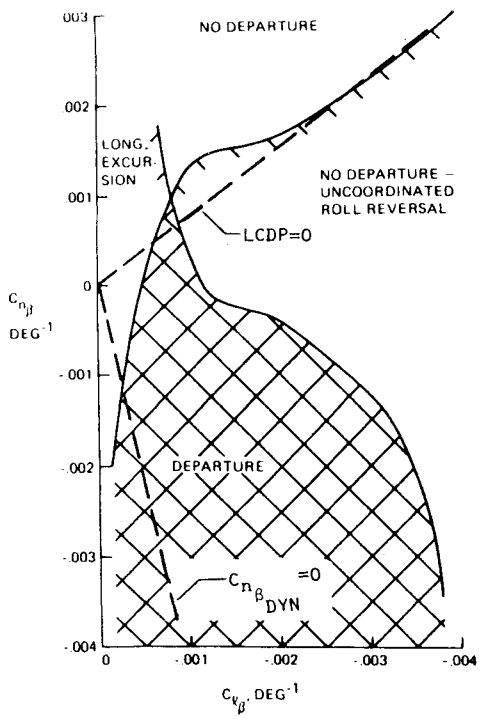

Fig. 13 Comparison of boundaries to LCDP and $C_{n_{\beta_{DYN}}}$ criteria for adverse $C_{n_{\delta_a}}$. $C_{n_{\beta_{DYN}}}$ based on $(I_z/I_x) = 6$ and $\alpha = 35$ deg.

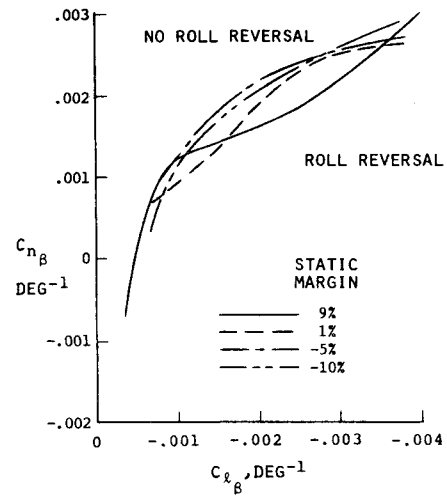

Fig. 14 Influence of static margin on uncoordinated roll-reversal boundary.

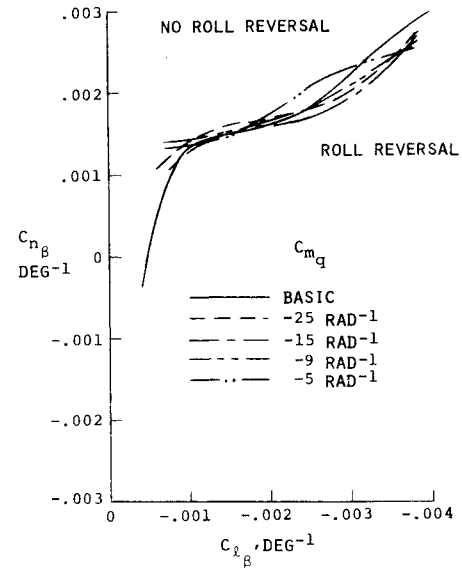

Fig. 15 Influence of C_{m_q} on uncoordinated roll-reversal boundary.

Comparison to Other Criteria

It is of interest to compare the boundaries discussed herein with other criteria, based on limited degree-of-freedom linearized equations, i.e., $C_{n_{\beta_{DYN}}}$ and LCDP. Consequently, plots of zero $C_{n_{\beta_{DYN}}}$ and LCDP were superimposed on the plots of Figs. 8-10 and are presented in Figs. 11-13 for proverse, neutral, and adverse $C_{n_{\delta_a}}$, respectively. As shown, $C_{n_{\beta_{DYN}}}$ is a nonconservative criterion when compared to the departure susceptibility boundary developed herein. Although $C_{n_{\beta_{DYN}}}$ predicts the stability of the dutch roll mode, it is insufficient as a departure criterion since it does not account for the lateral control characteristics (hence the identical $C_{n_{\beta_{DYN}}}$ curves in Figs. 11-13), and for aerodynamic and inertial coupling with the longitudinal motion. LCDP, however, appears to be a useful and accurate tool for predicting uncoordinated roll reversal, but *not* departure susceptibility.

Pitching Moment Effects

The investigation of the effect of pitching moment characteristics on the developed boundaries for an adverse

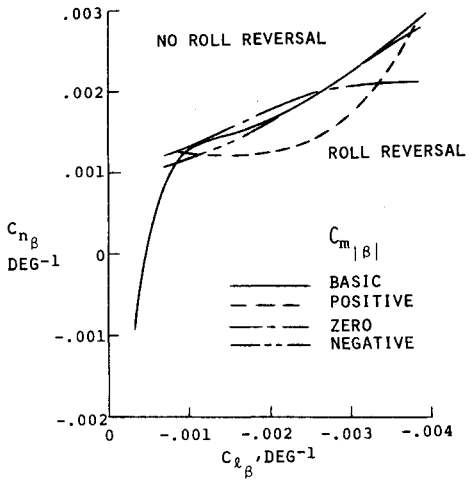

Fig. 16 Influence of $C_{m_{|\beta|}}$ on uncoordinated roll-reversal boundary.

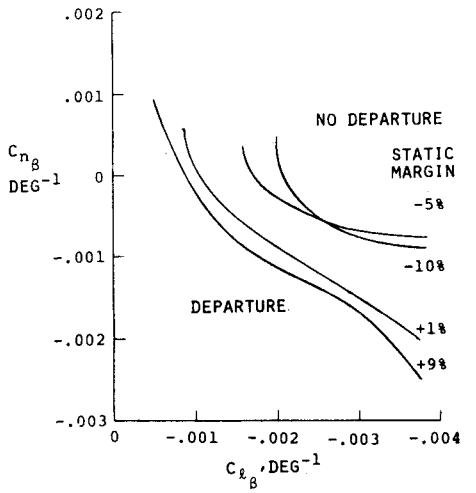

Fig. 17 Influence of static margin variations on departure susceptibility boundary.

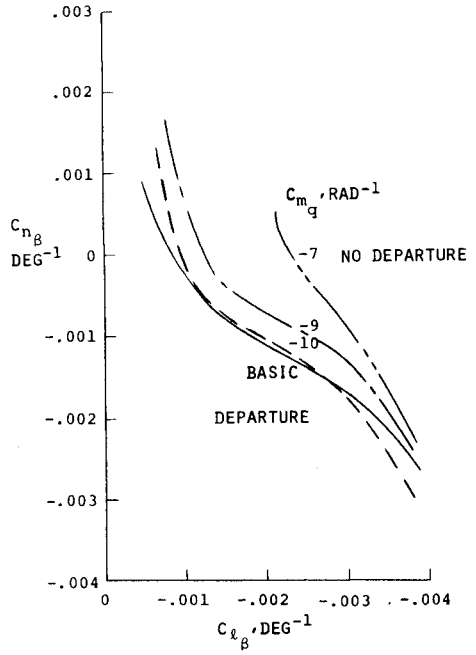

Fig. 18 Influence of C_{m_q} variations on departure susceptibility boundary.

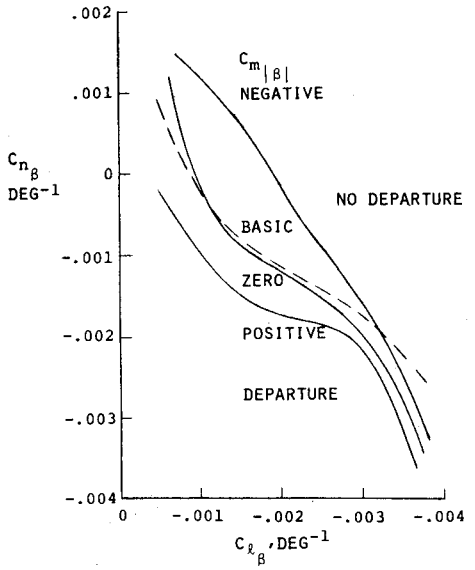

Fig. 19 Influence of $C_{m_{|\beta|}}$ variations on departure susceptibility boundary.

$C_{n_{\delta_a}}$ model demonstrated the following:

1) The uncoordinated roll reversal boundary was not pronouncedly influenced by any of the pitching moment parameters investigated and may be applied to any fighter configuration, as demonstrated by Figs. 14-16.

2) The developed departure susceptibility boundary would be applicable to most fighter configurations that exhibit static longitudinal stability, as shown in Fig. 17. Reducing the static margin from +9 to +1% resulted in only a very minor shift in the boundary. However, as the static margin became negative (unstable), increasingly more stringent requirements were placed on the high-angle-of-attack lateral-directional stability to avoid departure susceptibility for unaugmented airframes.

3) The departure susceptibility boundary would be nonconservative for unaugmented airframes with low C_{m_q} (less negative than -10 rad^{-1}) or unusual $C_{m_{|\beta|}}$ characteristics (large negative $C_{m_{|\beta|}}$ at high poststall angles of attack), as shown in Figs. 18 and 19, respectively.

Design Information

The following can be seen from the presented boundaries:

1) Positive directional stability at high alpha prevents an airplane performing a *severe* air combat maneuver from diverging to alphas above trim and into the region where spins are encountered, regardless of the level of dihedral effect and the value of $C_{n_{\delta_a}}$. It is the most effective parameter governing departure prevention.

2) For directionally unstable configurations, a large dihedral effect (negative C_{l_β}) can avert departure. However, this may require rolls to be coordinated to avoid roll reversal.

3) The presence of a proverse $C_{n_{\delta_a}}$ characteristic minimizes the value of C_{n_β} and C_{l_β} required to avoid departure or uncoordinated roll reversal.

Concluding Remarks

By using the boundaries presented herein, a fighter's response to a severe application of controls can be predicted as a function of its static lateral-directional stability and lateral control characteristics. The maneuver chosen for boundary development was purposely severe to conservatively identify combinations of the studied parameters that result in departure susceptibility. Less aggressive control inputs might not cause departure, but the potential would still be present. The boundaries appear to be applicable for most fighter mass

distributions and for a large range of pitch characteristics. They should, therefore, be useful for design tradeoff studies, airplane evaluation, and specification purposes.

Comparison of these results to the LCDP criterion indicates that a zero LCDP locus is a simple and accurate method for identifying uncoordinated roll reversal. $C_{n_{\beta_{DYN}}}$, however, appears to be a nonconservative predictor of departure susceptibility.

Acknowledgments

Studies reported herein were supported by NADC and AFFDL under Contracts N62269-77-C-0106 and F33615-78-C-3600, respectively.

References

[1] Bihrle, W. Jr. and Meyer, R.C., "F-14A High Angle-of-Attack Characteristics," *Journal of Aircraft,* Vol. 13, Aug. 1976, pp. 576-583.

[2] Bihrle, W. Jr. and Bowman, J.S. Jr., "Influence of Wing, Fuselage, and Tail Design on Rotational Flow Aerodynamics Beyond Maximum Lift," *Journal of Aircraft,* Vol. 18, Nov. 1981, pp. 920-925.

[3] Bihrle, W. Jr., "Influence of the Static and Dynamic Aerodynamic Characteristics on the Spinning Motion of Aircraft," *Journal of Aircraft,* Vol. 8, Oct. 1971, pp. 764-768.

[4] Moul, M.T. and Paulson, J.W., "Dynamic Lateral Behavior of High Performance Aircraft," NACA RM L58E16, Aug. 1958.

[5] Chambers, J.R., "Overview of Stall/Spin Technology," AIAA Paper 80-1580, Aug. 1980.

[6] Weissman, R., "Status of Design Criteria for Predicting Departure Characteristics and Spin Susceptibility," *Journal of Aircraft,* Vol. 12, Dec. 1975, pp. 989-993.

[7] Bihrle, W. Jr. and Barnhart, B., "Design Charts and Boundaries for Identifying Departure Resistant Fighter Configurations," NADC-76154-30, July 1978.

[8] Bihrle, W. Jr. and Barnhart, B., "Influence of Pitching Moment Characteristics on Departure and Uncoordinated Roll Reversal Boundaries for Fighter Configurations," AFFDL-TR-79-3157, Feb. 1980.